Biosensors and Bioelectronics 129 (2019) 36–41

Contents lists available at ScienceDirect

Biosensors and Bioelectronics

journal homepage: www.elsevier.com/locate/bios

# Signal-on electrochemiluminescence aptasensor for bisphenol A based on hybridization chain reaction and electrically heated electrode

Huifang Zhang[a,b], Fang Luo[a], Peilong Wang[c,*], Longhua Guo[a], Bin Qiu[a], Zhenyu Lin[a,*]

[a] MOE Key Laboratory for Analytical Science of Food Safety and Biology, Fujian Provincial Key Laboratory of Analysis and Detection Technology for Food Safety, Institute of Nanomedicine and Nanobiosensing, College of Chemistry, Fuzhou University, Fuzhou, Fujian 350116, China

[b] School of Chemistry and Chemical Engineering, Key Laboratory of Organo-pharmaceutical Chemistry of Jiangxi Province, Gannan Normal University, Ganzhou, 341000, P.R. China.

[c] Key Laboratory of Agrifood Safety and Quality, Ministry of Agriculture, Institute of Quality Standards & Testing Technology for Agriculture Products, China Agricultural Academy of Science, Beijing 100081, P.R. China

ARTICLE INFO

*Keywords:*
Electrochemiluminescence
Heated indium-tin-oxide electrode
Hybridization chain reaction
Aptamer
Bisphenol A

ABSTRACT

A simple and sensitive electrochemiluminescence (ECL) aptasensor has been developed for bisphenol A (BPA) detection. The capture DNA (CDNA) was modified on the heated indium-tin-oxide (ITO) working electrode surface firstly and then hybridized with BPA aptamer to form double strand DNA (dsDNA). The presence of target can cause the releasing of aptamer from the electrode surface since the aptamer prefers to switch its configuration to combine with BPA. Subsequently, the free CDNA will induce hybridization chain reaction (HCR) to produce long dsDNA on the electrode surface. $Ru(phen)_3^{2+}$ can integrate into the grooves of dsDNA to act as an ECL reagent, thus enhanced ECL signal can be detected. The temperature control during the processes of target recognition and HCR were realized through the heated electrode instead of the bulk solution heating. Furthermore, the performance of the ECL aptasensor can be further enhanced at elevated electrode temperature. Under the optimized conditions, the ECL intensity of the system has a linear relationship with the logarithm of BPA concentration in the range of 2.0 pM-50 nM. The limit of detection (LOD) at 55 °C (electrode surface temperature) was calculated to be 1.5 pM, which was approximately 6.5-fold lower than that at 25 °C. The proposed biosensor has been applied to detect the BPA in drink samples with satisfactory results.

## 1. Introduction

Bisphenol A (BPA), a key monomer for the polymer or related products, is considered as the most important endocrine disruptor that can lead to negative effects on human health in low dosage (Abnous et al., 2018; Lim et al., 2017). Many techniques had been developed and applied for BPA detection with high sensitivity (Shi et al., 2018). Gas chromatography mass spectrometry (GC-MS) and liquid chromatography mass spectrometry (LC-MS) are regarded as gold standard tools for BPA detection with excellent accuracy, but most of these methods need complicated sample preparation (Badie Bostan et al., 2017). Enzyme-linked immunosorbent assay (ELISA), fluorescence, and electrochemistry techniques had been applied to detect BPA also (Cao et al., 2014; Najafi et al., 2014; Zhou et al., 2013). Although the ELISA method has high selectivity, antigen and antibody used are relatively expensive. The fluorescence and electrochemistry methods are of high sensitivity, however, poor selectivity can be obtained (X. Guo et al., 2016), which must be coupled with other methods to resolve this problem. Electrochemiluminescence (ECL), combines the characters of electrochemistry and luminescence, has the advantages of simple instrument and high sensitivity (Chen et al., 2011; Liu et al., 2011). Recently, this technique had been used to detect BPA with high sensitivities. For example, Zhuang et al. established an ECL sensor for BPA determination based on the inhibition of luminol-dissolved oxygen ECL system through the addition of BPA (Zhuang et al., 2008). The quenching effect of BPA on the ECL performance of peroxydisulfate solution had been applied to develop ECL sensor for BPA detection also (W. Guo et al., 2016). However, the selectivity of these two methods is not high enough. Recently, our group combines the advantages of ECL and high selectivity of molecular imprinted technique (MIP) to develop a selective BPA sensor (Lin et al., 2016). Nevertheless, the previous preparation for MIP seems to be tedious and low sample-load capacity may be obtained (Li and Row, 2018). Aptamer possesses the advantages of high binding affinity, cost-effectiveness, and superior specificity. Some aptamer-based ECL sensors for BPA had been developed with higher selectivity. For example, an aptamer-based ECL sensor using

* Corresponding authors.
*E-mail addresses:* wangpeilong@caas.cn (P. Wang), zylin@fzu.edu.cn (Z. Lin).

https://doi.org/10.1016/j.bios.2019.01.007
Received 1 October 2018; Received in revised form 7 January 2019; Accepted 7 January 2019
Available online 15 January 2019
0956-5663/ 

$Mn^{2+}$-doped $NaYF_4$:Yb/Er upconversion nanoparticles as ECL reagent was successfully developed for BPA detection (X. Guo et al., 2016). Yet the synthesis of the ECL reagent is difficult, and the labeling step of the ECL reagent on the DNA is complex. $Ru(phen)_3^{2+}$, as a relatively common ECL reagent, can be embedded into the grooves of double strand DNA (dsDNA) with high efficiency, which enabled the construction of label-free ECL biosensors (Carter and Bard, 1990). In an early study, we developed a signal-off ECL aptasensor for BPA using $Ru(phen)_3^{2+}$ as the signal indicator (Ye et al., 2017). However, the signal-off model may reach possible false-positive results (Han et al., 2016). Therefore, the signal-on strategy is more reliable for sensitive BPA detection.

Electrically heated electrodes have gained increasing attention on its quick, versatile and convenient means to adjust the temperature desired (Gründler et al., 1993; Walter et al., 2016). The major character of this technique lies in that the temperature of the electrode can be heated up quickly while leaving the bulk solution at ambient temperature, which promoted the performance of the sensor by affecting thermodynamic and kinetic parameters of the reaction (Wu et al., 2013). Early report indicated that the temperature changing adjusted by an electrically heated electrode can be used to control the DNA interactions with improved hybridization efficiency (Jacobsen and Flechsig, 2013). Researchers also demonstrated that the electrode surface temperature affected the ECL behavior of $Ru(bpy)_3^{2+}$ greatly and suitable electrode surface temperature (adjusted by electrically heated cylindrical microelectrode) can be chosen to improve the performance of the sensor (Lin et al., 2006). Our recent study further confirmed that the electrically heated electrode can be used to control the suitable temperature need for DNA hybridization and enzyme action (Zhang et al., 2018). On the basis of these results, the superior property of heated electrode for in situ temperature control and signal enhancement can be decided.

Hybridization chain reaction (HCR) is a triggered self-assembly and enzyme-free process (Dirks and Pierce, 2004). This technology enables the cascade of hybridization events with high amplification capability and long dsDNA can be formed eventually (Huang et al., 2011). The produced dsDNA can be served as the carrier for the intercalation of $Ru(phen)_3^{2+}$ to obtain a strong ECL signal. In a traditional HCR, the temperature needs to be controlled carefully for a better amplification efficiency (Wang et al., 2015), which is normally realized through bulk solution heating, the procedure is tedious and time-consuming. In this study, a signal-on ECL aptasensor for BPA has been developed through coupling the advantages of the electrically heated electrode and the signal amplification strategy of HCR. The temperatures needed during the process of aptamer-target interactions, DNA hybridization etc. have been controlled accurately and easily by the electrically heated electrode instead of the bulk solution heating. $Ru(phen)_3^{2+}$ has been intercalated into the grooves of dsDNA and acted as the ECL probe (Chen et al., 2009), which overcome the troublesome modification of ECL indicator on DNA in the conventional strategies. The ECL response of the system has been further improved at elevated electrode surface temperature. The proposed biosensor has also been applied to detect BPA in drinks samples with satisfactory results.

## 2. Experimental section

### 2.1. Reagents

Dichlorotris (1,10-phenanthroline) ruthenium(II) hydrate ($Ru(phen)_3^{2+}$), Chloroauric acid tetrahydrate ($HAuCl_4{\cdot}4H_2O$) and $K_3Fe(CN)_6$ were brought from Sinopharm Chem. Re. Co., Ltd. (Shanghai, China). BPA, Bisphenol S (BPS), Bisphenol F (BPF), progesterone (PRG) and Hydroquinone (HQ) were acquired from Sigma-Aldrich (St. Louis, MO, USA). Dimethyl Sulfoxide (DMSO), Tripropylamine (TPA), tris (2-carboxyethyl) phosphine (TCEP) and 6-mercaptohexanol (MCH) were purchased from Aladdin (Shanghai, China), SYBR Green I (10000 ×) was purchased from Solarbio (Beijing, China). BPA (0.0091 g) was dissolved in 2 mL DMSO to make 20 mM BPA stock solution. BPA binding buffer: 20 mM Tris-HCl, 100 mM NaCl, 25 mM KCl, 10 mM $MgCl_2$, and 5% DMSO, pH 8.0.

The specific oligonucleotides used in this strategy were synthesized by Sangon Inc. (Shanghai, China) and the sequences were shown as follows: (5′-3′)

Capture DNA (CDNA): SH-TTT TTT TTT TCG TGA TGC GCT GGG CCA TAC GCG GAA CGC TAT

BPA aptamer: CCG GTG GGT GGT CAG GTG GGA TAG CGT TCC GCG TAT GGC CCA GCG CAT CAC GGG TTC GCA CCA

Hairpin 1 (HP1): GCT GGG CCA TAC GCG GAA CGC TAT ATA GCG TG A TAG CGT TCC GCG TAT GGC CCA GCG CAT CAC G

Hairpin 2 (HP2): CAC GCT ATA TAG CGT TCC GCG TAT GGC CCA GCC GTG ATG CGC TGG GCC ATA CGC GGA ACG CTA T

### 2.2. Instrument

The electrochemical and ECL measurements were carried out with an electrochemical workstation (CHI 660D, CH Instruments, USA) and a BPCL Ultra-Weak Luminescence Analyzer (Institute of Biophysics, Chinese Academy of Science, Beijing, China), respectively. A function generator (DF1636A, Zhongce Electronics Co., Ltd., Ningbo, China) equipped with a transformer was used for electrically heating. An electrically heated indium-tin-oxide (ITO) working electrode (2 cm × 2 cm slice with a T-shape ITO membrane of 4 mm in width; Xiangcheng Technology Co., Shenzhen, China), a platinum wire and an Ag/AgCl electrode worked as the working electrode, counter electrode, and reference electrode, respectively. The fluorescence measurements were performed on a Hitachi F-7000 spectrofluorimeter (Hitachi, Tokyo, Japan).

Construction of the heated ITO electrode was referred to the early report (Chen et al., 2009), and the temperature was calibrated by open circuit potentiometry (Chen et al., 2009; Zerihun and Gründler, 1996). Briefly, two similar ITO electrodes were placed into two separate solutions of 10 mM $[Fe(CN)_6]^{3-/4-}$ in 0.5 M KCl and connected with a salt bridge. By controlling in the change of temperature in the one solution, open circuit potential of the reversible redox couple was varying. Thus, the temperature coefficient of the electrode potential could be obtained. Subsequently, the relationship between the electrode potential with the applied heating voltages was investigated through the application of various heating voltages in the one electrode. Based on the results mentioned above, the relationship between the heating voltages and the temperature of electrode surface could be deduced.

### 2.3. HCR amplification and ECL detection

Before the experiment, the bare ITO was subjected to cyclic voltammetry (CV) measurement (from −0.4 to +0.6 V) in $HAuCl_4$ (0.5 mM) to form a gold film on the electrode surface. CDNA (1 μM) was modified on the electrode surface through the Au-S covalent bond. MCH was then utilized to block the unoccupied sites. Subsequently, Tris-HCl buffer (50 mM, pH = 7.4) containing 1 μM BPA aptamer was added to form dsDNA at the electrode surface temperature of 37 °C. After that, the electrodes were immersed in different concentrations of BPA (diluted by the binding buffer) and incubated for 80 min in the same condition. Next, HCR was carried out at 37 °C for 100 min when the electrode was soaked in the solution containing HP1 (2 μM), HP2 (2 μM) and Tris-HCl buffer (10 mM, pH = 7.4). Finally, the modified electrode was immersed in $Ru(phen)_3^{2+}$ (1 mM) solution and incubated for 3.5 h at room temperature. It is noteworthy that the electrode was rinsed repeatedly after each step. ECL detection was performed in

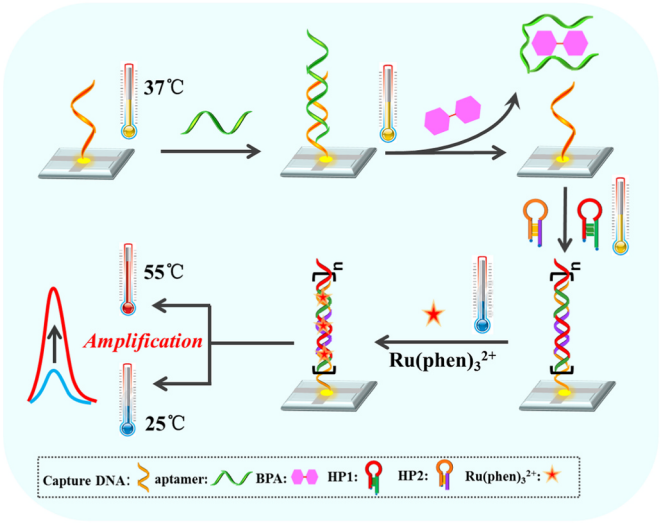


**Scheme 1.** Illustration of the signal-on ECL aptasensor for in situ detection of BPA based on HCR and electrically heated ITO electrode.

phosphate buffer (PBS, 10 mM, pH 7.4) containing 20 mM TPA and the electrode was electrically heated to an appreciate temperature.

## 3. Results and discussion

### 3.1. Principle of the proposed ECL aptasensor for BPA

Scheme 1 showed the principle of the proposed ECL aptasensor for BPA detection. The electrically heated ITO electrode not only acts as the working electrode but also serves as the carrier and temperature controller for aptamer-target binding and DNA interaction in this system. Thiolated CDNA has been immobilized on the electrode surface via Au-S covalent bonds firstly. Then BPA aptamer was partly hybridized with CDNA at the electrode surface temperature of 37 °C. In the presence of target (BPA in this study), the aptamer prefers to switch its configuration to combine with BPA (Ding et al., 2015; Jo et al., 2011; Li et al., 2016). Therefore, the CDNA become free again on the electrode surface. In this stage, two hairpin probes (HP1 and HP2) were employed to react with the free CDNA at the electrode temperature of 37 °C. Briefly, CDNA pairs with the sticky end of H1 and opens it through strand-displacement interaction. The newly exposed sticky end of H1 then opens H2 in a similar way to form a sticky end identical in sequence to CDNA. Repeat the above procedure, a long chain-like dsDNA can be produced through the HCR reaction (Wang et al., 2015). Ru(phen)$_3^{2+}$ can embed into the grooves of dsDNA and act as the ECL indicator (Tang et al., 2010), so relative large ECL intensity can be detected. However, in the absence of BPA, the CDNA was restricted by aptamer and was not able to trigger the process of HCR, only short dsDNA presented on the electrode surface (formed between CDNA and aptamer). Therefore, little Ru(phen)$_3^{2+}$ was modified on the electrode, and low ECL response was detected. Based on this, a signal-on ECL aptasensor for BPA can be developed. Since the electrode surface temperature affected the ECL behavior of Ru(phen)$_3^{2+}$ greatly (Chen et al., 2007; Lin et al., 2006), the performance of the proposed sensor can be further improved by adjusting the electrode surface temperature to appropriate level.

### 3.2. Feasibility analysis

Uncoiling of double helix due to the BPA binding is a critical point to achieve highly sensitive and selective detection. A fluorescence measurement was performed to demonstrate the disassembly of the CDNA-aptamer structure when BPA was added. It is well known that SYBR Green I can bind to the groove of dsDNA and exhibit fluorescence enhancement (Lin et al., 2018). Consequently, uncoiling of DNA double helix due to the BPA binding would reduce the fluorescence. As shown

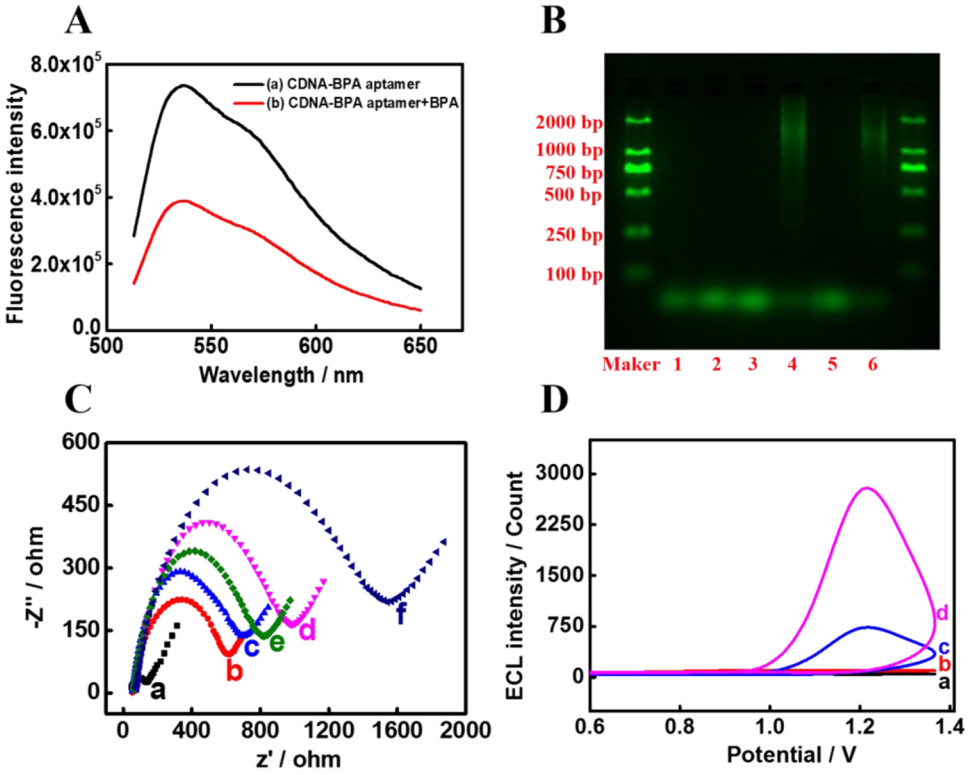


**Fig. 1.** (A). Fluorescence emission spectroscopy of the proposed method with and without BPA: 100 nM CDNA + 100 nM BPA aptamer (curve a); 100 nM CDNA + 100 nM BPA aptamer +100 μM BPA (curve b); [SYBR Green I] = 0.5 ×. (B) AGE results of the designed system. Lane 1:1 μM HP1; lane 2: 1 μM HP2; lane 3: mixture of HP1 and HP2 (final concentration 1 μM); lane 4: CDNA with the mixture of 1 μM HP1 and 1 μM HP2; lane 5: lane 4 + BPA aptamer; lane 6: lane 5 + BPA. (C) Nyquist diagrams of (a): Au modified ITO electrode; (b): CDNA modified electrode; (c): b + MCH; (d): c + BPA aptamer; (e): d + BPA; (f): after HCR. The frequency ranges from 100k Hz to 0.01 Hz. (D) ECL response in the absence of BPA at 25 °C (curve a) and 55 °C (curve b); ECL response in the presence of 100 pM BPA at 25 °C (curve c) and 55 °C (curve d) with the heated ITO electrode. TPA: 20 mM in PBS (pH 7.4); scan rate 0.1 V/s.

in Fig. 1A, a strong fluorescence signal was observed in the control group (curve a) due to the hybridization of CDNA and BPA aptamer. After the addition of BPA, the fluorescence intensity diminished (curve b). This means the amount dsDNA in the solution decreased, which verified our assumption.

The product of HCR served as the carrier of $Ru(phen)_3^{2+}$ for signal collection, therefore agarose gel electrophoresis (AGE) was applied to verify the successful HCR firstly (Chang et al., 2016). As shown in Fig. 1B, only low molecular weight bands were observed in lane 1 (HP1), lane 2 (HP2) and line 3 (the mixture of the two hairpins). Once CDNA was introduced, smears of high molecular weight bands were observed, indicating the production of long length dsDNA presented (lane 4). However, a combination of BPA aptamer and CDNA firstly would hinder the reaction of HCR, causing the invisibility of the smears (lane 5). After the addition of BPA into the system, the aptamer preferred to form BPA-aptamer complex in lieu of aptamer-CDNA duplex, so CDNA became free again and the long length of dsDNA formed (lane 6). These results indicate that the HCR process occurred in the presence of BPA

Electrochemical impedance spectroscopy (EIS) has been applied to demonstrate the reliability of the proposed mechanism also (carried out by alternating current impedance measurements in KCl solution (0.5 M) containing $[Fe(CN)_6]^{3-/4-}$ (10 mM) at an amplitude of 5 mV). The semicircle domain at high frequencies in the Nyquist diagrams was consistent with the electron transfer resistance (Zhang et al., 2008). As shown in Fig. 1C, a very small semicircular domain was obtained from the Au-modified ITO electrode (curve a), indicating that the electron transported easily to the ITO electrode. After the immobilization of CDNA, the semicircular domain became large due to the effect of electrostatic repulsion between the negative charged CDNA and $[Fe(CN)_6]^{3-/4-}$ (curve b). The impedance further increased when the electrode was blocked by MCH (curve c). The semicircular domain increased significantly due to the hybridization of aptamer and CDNA (curve d). However, the impedance decreased later after the incubation with BPA (100 pM), probably because the aptamer was released from the electrode surface (curve e). But after the HCR reaction, the semicircle domain of impedance enlarged greatly again (curve f), which indicated that long chain-like dsDNA has been accumulated on the surface of the ITO electrode.

ECL performance in the presence and absence of BPA were investigated too. As shown in Fig. 1D, in the absence of BPA, the ECL signal was weak at the electrode surface temperature of 25 °C (curve a) during the ECL detection. When the temperature increased to 55 °C, the ECL intensity of the system changed little (curve b). However, a strong ECL response could be detected in the presence of BPA (100 pM) at the electrode surface temperature of 25 °C (curve c). And the ECL intensity enhanced greatly when the temperature was adjusted to 55 °C (curve d), which verified that better ECL performance can be achieved at the elevated electrode temperature. These results demonstrate the feasibility of the proposed biosensor.

### 3.3. Optimization of experimental conditions

A series of experimental conditions that affected the performance of the proposed ECL system were optimized. The reaction time between BPA and its specific aptamer affected the amount of single CDNA presented on the electrode surface greatly, thus this parameter was optimized firstly. As illustrated in Fig. 2A, ECL signal increased with the increasing reaction time between BPA and aptamer and reached a plateau after 80 min. Therefore 80 min was chosen as the optimum conditions. The self-assembly time of HCR affects the amount of dsDNA produced, which in turn affects the amount of $Ru(phen)_3^{2+}$ embedded. The results indicated that the ECL signal increased gradually with the increasing reaction time of HCR and little increasing had been detected after 100 min (Fig. 2B). Therefore, 100 min had been chosen as the best condition for the subsequent experiments. Similar to the trend in HCR reaction time, the ECL intensity increased with the extension of interaction time between $Ru(phen)_3^{2+}$ and dsDNA on the electrode surface, and nearly no further enhancement had been observed after 3.5 h. Therefore, 3.5 h of $Ru(phen)_3^{2+}$ intercalation time was finally selected as the optimum condition (Fig. 2C). The hairpin probe plays an important role in the amplification process, thus the concentration of H1 and H2 was optimized (the H1/H2 molar ratio was controlled to be 1:1). As shown in Fig. 2D, the ECL signal increased with the increasing concentration of H1 and H2 and reached a plateau after 1 μM. Therefore, 1 μM of H1 and H2 were used for the assay. Aptamer also has a great influence on the background noise of the system, therefore, the influence of aptamer concentration on the ECL signal was further investigated. As shown in Fig. 2E, the ECL signal decreased with the increasing concentration of BPA aptamer and reached a plateau after 1 μM approximately. Therefore, 1 μM aptamer was chosen for the following assay.

Effect of the electrode surface temperature on the ECL behavior of immobilized $Ru(phen)_3^{2+}$ was studied too. As shown in Fig. 2F, the ECL signal increased with the increasing electrode temperature from 25 °C to 55 °C (red line), while little effect on the background signal was observed (black line). The ECL signal at 55 °C was approximately 4 times than that at 25 °C, the reason lies in that a temperature gradient layer near the electrode surface can be formed at high electrode surface temperature, which will speed up the diffusion and convection of the electrode active compounds to the electrode surface (Lin et al., 2010). However, the ECL signal decreased and a major disturbance in the background noise was observed when the temperature was over 55 °C, which may attribute to the lower quantum efficiency of $Ru(phen)_3^{2+}$ at a higher temperature (Lin et al., 2009), and the destruction of the self-assembled probe on the electrode surface (Flechsig et al., 2005). Hence, 55 °C was chosen for subsequent experiments.

### 3.4. Analytical performance of the proposed aptasensor

Fig. 3A showed the ECL response of the system with different concentrations of BPA under the optimized experimental conditions. The ECL signal increased with the increasing concentration of BPA at the electrode surface temperature of 55 °C. The ECL intensity ($I$) has a linear relationship with logarithm (lg) of BPA concentration in the range of 2.0 pM-50 nM (curve a in Fig. 3B) with the following equation: $I = 1446.8 \lg(BPA) + 4019.1$ ($R^2 = 0.9944$). If the electrode temperature changed to 25 °C, the linear range changed to 0.01–50 nM and the equation was: $I = 336.1 \lg(BPA) + 981.8$ ($R^2 = 0.9886$). The limit of detection (LOD, S/N = 3) at 55 °C was calculated to be 1.5 pM, which was approximately 6.5-fold lower than that at 25 °C (curve b in Fig. 3B) due to the impact of signal enhancement of heated ITO electrode. Moreover, compared to the previously reported aptamer-based sensors, the proposed method enables the higher sensitivity and wider detection range for BPA detection (Table S1).

The specificity of the developed aptasensor was evaluated. Four different structural analogs, including PRG, HQ, BPS and BPF, had been chosen as the potential interference. As shown in Fig. 4A, weak ECL signals had been detected in the presence of high concentration of interfering substances (100 nM) (nearly the same as the background signal). But when the target existed (100 pM), a strong ECL signal had been detected. In addition, the presence of the inorganic ions such as $Na^+$, $K^+$, $Ca^{2+}$, $Cu^{2+}$ had a scarce influence on the detection of BPA either (data not shown). These results demonstrated the proposed aptasensor has good specificity towards BPA detection.

Reproducibility was evaluated through three parallel determinations at different electrode temperatures (the concentration of BPA was 100 pM). The results demonstrated that the relative standard deviation (RSD) were 5.3%, 4.1%, and 2.6% at the temperature of 25, 37 and 55 °C, respectively (shown in Fig. 4B), which indicated that better reproducibility can be obtained at elevated electrode temperature. Fig. S1 shows the response for repetitive measurement of 100 pM BAP under

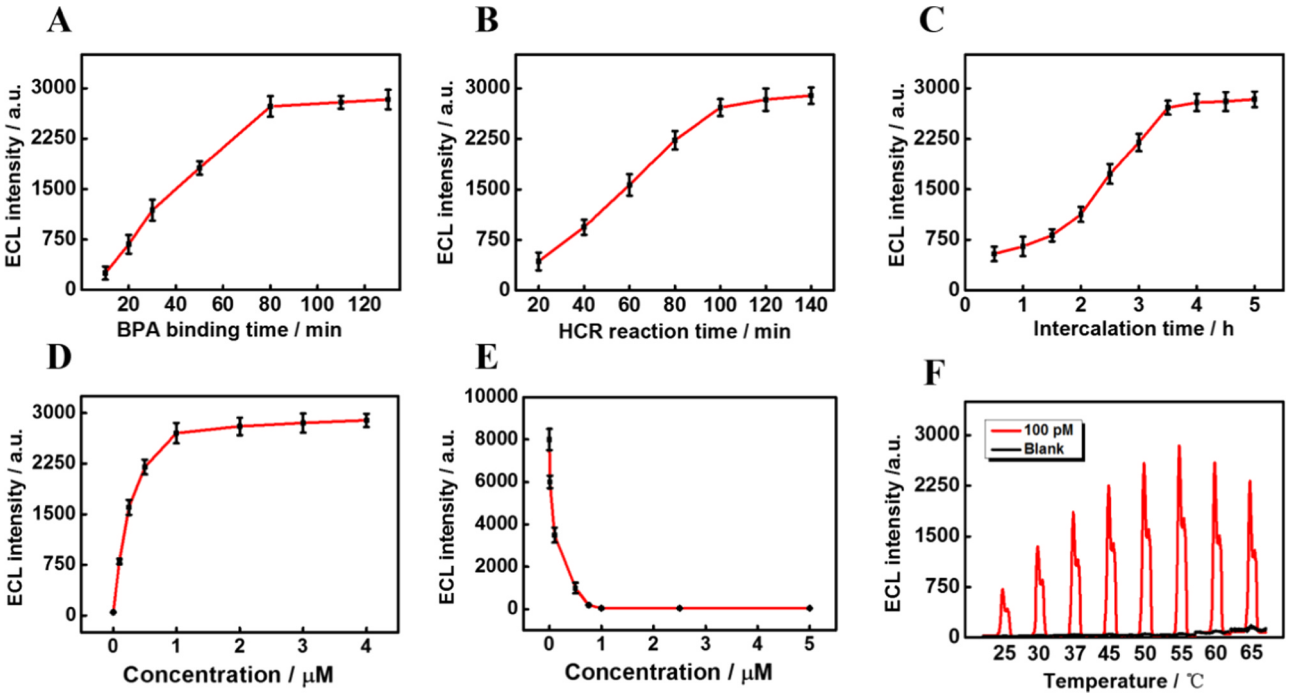


**Fig. 2.** Effects of (A) the reaction time between BPA and its aptamer, (B) self-assembly time of HCR, (C) the intercalation time between $Ru(phen)_3^{2+}$ and dsDNA, (D) the concentration of H1/H2 (condition: [H1]:[H2] = 1:1), and (E) the concentration of BPA aptamer on the ECL performance of the system. (F) The effect of the electrode surface temperature on the performance of the system. BPA:100 pM; TPA: 20 mM in PBS (pH 7.4); scan rate 0.1 V/s (For interpretation of the references to color in this figure, the reader is referred to the web version of this article.).

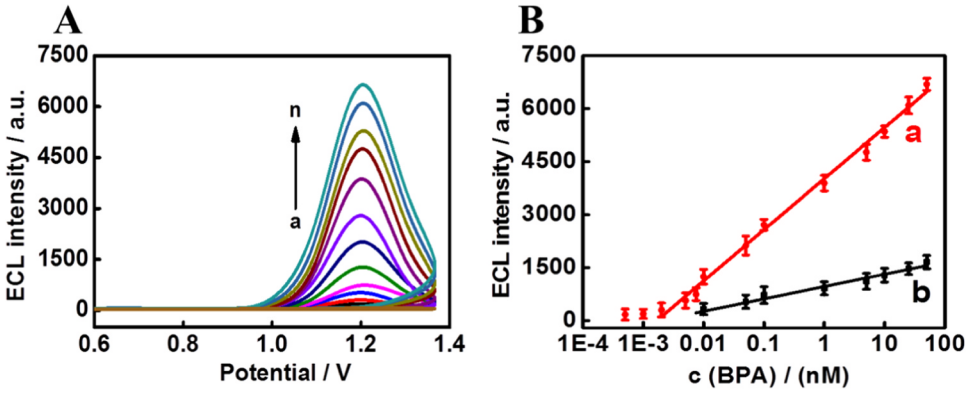


**Fig. 3.** (A) ECL signals with different concentrations of BPA (a-n: 0, 0.5 pM, 1 pM, 2 pM, 5 pM, 7.5 pM,10 pM, 50 pM, 100 pM, 1 nM, 5 nM, 10 nM, 25 nM, 50 nM) at the electrode temperature of 55 °C. (B) The relationship between ECL intensity and the BPA concentration at different electrode temperature (a) 55 °C; (b) 25 °C. TPA: 20 mM in PBS (pH 7.4); scan rate 0.1 V/s.

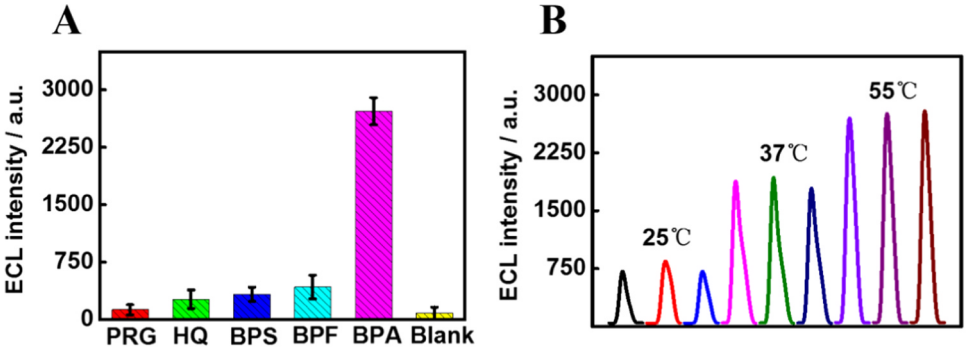


**Fig. 4.** (A) Specificity investigation for target BPA against other structural analogs of PRG, HQ, BPS, and BPF. (B) ECL reproducibility of the developed aptasensor at different electrode temperatures. TPA: 20 mM in PBS (pH 7.4); scan rate: 0.1 V/s.

**Table 1**
Detection of BPA in drinks samples by the proposed sensor in comparison to LC-MS.

| Samples | | Detected (nM) | Spiked (nM) | Detected after addition (nM) | Detectedby LC-MS (nM) | Recovery rates (%) | RSD (%) |
|---|---|---|---|---|---|---|---|
| Milk | 1 | – | 1 | 1.05 | 1.02 | 105 | 5.2 |
| | 2 | – | 5.0 | 4.92 | 4.96 | 98.4 | 3.8 |
| | 3 | – | 10.0 | 9.91 | 9.88 | 99.1 | 4.4 |
| Orange Juice | 1 | – | 1 | 0.96 | 0.99 | 96.0 | 4.7 |
| | 2 | – | 5.0 | 5.06 | 5.02 | 101.2 | 5.3 |
| | 3 | – | 10.0 | 9.88 | 10.04 | 98.8 | 6.1 |
| Coconut Juice | 1 | – | 1 | 1.03 | 0.97 | 103 | 5.2 |
| | 2 | – | 5.0 | 5.04 | 5.06 | 100.8 | 3.9 |
| | 3 | – | 10.0 | 9.73 | 9.85 | 97.3 | 5.7 |

"–" means no BPA was detected.

continuous potential scaning. The ECL response tended to level off with an RSD of 3.1%, which also indicated that the proposed method has good stability.

### 3.5. Application of proposed ECL aptasensor

The proposed aptasensor has been applied to detect BPA in drinks (milk, orange juice, and coconut juice) samples later. The samples were treated according to the early reported literature firstly (Zhou et al., 2014). Moreover, standard addition recoveries had been studied to further verify the accuracy of the proposed method. As shown in Table 1, none detectable BPA was presented in these samples. The standard addition recoveries were in the range of 98.4–105% in milk, 96.0–101.2% in orange juice, and 97.3–103% in coconut juice, respectively. The outcomes are in good accordance with that detected by LC-MS analysis (Inoue et al., 2003). These results demonstrated that the proposed aptasensor can be used to detect BPA in real samples with satisfying results.

## 4. Conclusion

In summary, a signal-on ECL aptasensor that combines the advantages of in situ temperature control by the electrically heated electrode and the high amplification efficiency of HCR has been successfully developed for BPA detection. The obtained results indicated that the electrode heating has the same effect as that of the bulk solution heating. Moreover, possible false-positive results caused by the signal-off model can be eliminated. Better performance of the ECL aptasensor can be further acquired with the electrically heated electrode, the LOD at 55 °C is approximately 6.5-fold lower than that at 25 °C. The proposed aptasensor has been applied to detect BPA in drink samples with satisfactory results. This work is simple, low-cost, label-free and high sensitive, which will enable the effective point of in-situ detection of different targets with sensitive measurements. Moreover, by changing the aptamer used, the proposed method can be expanded to detect other targets easily.

## Acknowledgment

This project was financially supported by National Key R&D Program of China (2017YFC1600303), NSFC (21777189, 21575025), the Program for Changjiang Scholars and Innovative Research Team in University (No. IRT15R11), the cooperative project of production and study in University of Fujian Province (2018Y4007), the Natural Science Foundation of Fujian Province (2018J01685, 2018J01682) and STS Key Project of Fujian Province (2017T3007).

## Appendix A. Supplementary material

Supplementary data associated with this article can be found in the online version at doi:10.1016/j.bios.2019.01.007.

## References

Abnous, K., Danesh, N.M., Ramezani, M., Alibolandi, M., Taghdisi, S.M., 2018. Biosens. Bioelectron. 119, 204–208.
Badie Bostan, H., Danesh, N.M., Karimi, G., Ramezani, M., Mousavi Shaegh, S.A., Youssefi, K., Charbgoo, F., Abnous, K., Taghdisi, S.M., 2017. Biosens. Bioelectron. 98, 168–179.
Cao, X., Shen, F., Zhang, M., Bie, J., Liu, X., Luo, Y., Guo, J., Sun, C., 2014. RSC Adv. 4 (32), 16597–16606.
Carter, M.T., Bard, A.J., 1990. Bioconj. Chem. 1 (4), 257–263.
Chang, C.-C., Chen, C.-Y., Chuang, T.-L., Wu, T.-H., Wei, S.-C., Liao, H., Lin, C.-W., 2016. Biosens. Bioelectron. 78, 200–205.
Chen, L., Huang, D., Ren, S., Chi, Y., Chen, G., 2011. Anal. Chem. 83 (17), 6862–6867.
Chen, Y., Jiang, Y., Lin, Z., Sun, J., Zhang, L., Chen, G., 2009. Analyst 134 (4), 731–737.
Chen, Y., Lin, Z., Chen, J., Sun, J., Zhang, L., Chen, G., 2007. J. Chromatogr. 1172 (1), 84–91.
Ding, J., Gu, Y., Li, F., Zhang, H., Qin, W., 2015. Anal. Chem. 87 (13), 6465–6469.
Dirks, R.M., Pierce, N.A., 2004. Proc. Natl. Acad. Sci. USA 101 (43), 15275–15278.
Flechsig, G.-U., Peter, J., Hartwich, G., Wang, J., Gründler, P., 2005. Langmuir 21 (17), 7848–7853.
Gründler, P., Zerihun, T., Möller, A., Kirbs, A., 1993. J. Electroanal. Chem. 360 (1), 309–314.
Guo, W., Zhang, A., Zhang, X., Huang, C., Yang, D., Jia, N., 2016a. Anal. Bioanal. Chem. 408 (25), 7173–7180.
Guo, X., Wu, S., Duan, N., Wang, Z., 2016b. Anal. Bioanal. Chem. 408 (14), 3823–3831.
Han, S., Zhou, X., Tang, Y., He, M., Zhang, X., Shi, H., Xiang, Y., 2016. Biosens. Bioelectron. 80, 265–272.
Huang, J., Wu, Y., Chen, Y., Zhu, Z., Yang, X., Yang, C.J., Wang, K., Tan, W., 2011. Angew. Chem. Int. Ed. 50 (2), 401–404.
Inoue, K., Murayama, S., Takeba, K., Yoshimura, Y., Nakazawa, H., 2003. J. Food Compos. Anal. 16 (4), 497–506.
Jacobsen, M., Flechsig, G.-U., 2013. Electroanalysis 25 (2), 373–379.
Jo, M., Ahn, J.-Y., Lee, J., Lee, S., Hong, S.W., Yoo, J.-W., Kang, J., Dua, P., Lee, D.-K., Hong, S., 2011. Oligonucleotides 21 (2), 85–91.
Li, G., Row, K.H., 2018. Sep. Purif. Rev. 47 (1), 1–18.
Li, X., Song, J., Xue, Q.-W., You, F.-H., Lu, X., Kong, Y.-C., Ma, S.-Y., Jiang, W., Li, C.-Z., 2016. Nanomaterials 6 (10), 190.
Lim, H.J., Chua, B., Son, A., 2017. Biosens. Bioelectron. 94, 10–18.
Lin, B., Yu, Y., Cao, Y., Guo, M., Zhu, D., Dai, J., Zheng, M., 2018. Biosens. Bioelectron. 100, 482–489.
Lin, Y., Cao, J., Li, X., Zhang, X., Zhang, J., Lin, Z., 2016. Anal. Methods 8 (41), 7445–7452.
Lin, Z., Chen, X., Chen, H., Qiu, B., Chen, G., 2009. Electrochem. Commun. 11 (10), 2056–2059.
Lin, Z., Sun, J., Chen, J., Guo, L., Chen, G., 2006. Anal. Chim. Acta 564 (2), 226–230.
Lin, Z., Wang, W., Jiang, Y., Qiu, B., Chen, G., 2010. Electrochim. Acta 56 (2), 644–648.
Liu, D.-Y., Xin, Y.-Y., He, X.-W., Yin, X.-B., 2011. Biosens. Bioelectron. 26 (5), 2703–2706.
Najafi, M., Khalilzadeh, M.A., Karimi-Maleh, H., 2014. Food Chem. 158, 125–131.
Shi, L., Rong, X., Wang, Y., Ding, S., Tang, W., 2018. Biosens. Bioelectron. 102, 41–48.
Tang, C.-X., Zhao, Y., He, X.-W., Yin, X.-B., 2010. Chem. Commun. 46 (47), 9022–9024.
Walter, A., Langschwager, F., Marken, F., Flechsig, G.-U., 2016. Sens. Actuators B 233, 502–509.
Wang, X., Jiang, A., Hou, T., Li, H., Li, F., 2015. Biosens. Bioelectron. 70, 324–329.
Wu, S.-H., Zhu, B.-J., Huang, Z.-X., Sun, J.-J., 2013. Electrochem. Commun. 28, 47–50.
Ye, S., Ye, R., Shi, Y., Qiu, B., Guo, L., Huang, D., Lin, Z., Chen, G., 2017. Anal. Bioanal. Chem. 409 (30), 7145–7151.
Zerihun, T., Gründler, P., 1996. J. Electroanal. Chem. 404 (2), 243–248.
Zhang, H., Zhuo, Z., Chen, L., Chen, C., Luo, F., Chen, Y., Guo, L., Qiu, B., Lin, Z., Chen, G., 2018. Electrochem. Commun. 88, 75–78.
Zhang, S., Xia, J., Li, X., 2008. Anal. Chem. 80 (22), 8382–8388.
Zhou, J., Zhao, S., Zhang, J., Zhang, L., Cai, Y., Zhou, L., 2013. Anal. Methods 5 (6), 1570–1576.
Zhou, L., Wang, J., Li, D., Li, Y., 2014. Food Chem. 162, 34–40.
Zhuang, Y.-F., Zhang, J.-T., Cao, G.-P., 2008. J. Chin. Chem. Soc. 55 (5), 994–1000.